15 May 2000

ELSEVIER

Optics Communications 178 (2000) 437–447

OPTICS COMMUNICATIONS

www.elsevier.com/locate/optcom

# Optimization of the process of frequency tripling and quadrupling in double grating quasi-phase matched structures

Yana Deyanova, Solomon Saltiel *, Kaloian Koynov

*Quantum Electronics Department, Faculty of Physics, University of Sofia, BG-1164, Sofia, Bulgaria*

Received 15 November 1999; received in revised form 20 February 2000; accepted 29 March 2000

**Abstract**

Monolithic nonlinear crystal with two quasi-phase matched gratings designed for third or fourth harmonic generation is investigated theoretically. The optimal lengths and the periods of the two quasi-phase matched gratings and also the temperature and wavelength acceptance are found. The efficiency of this double-grating frequency monolithic converter is compared with the efficiency of the converter that uses nonlinear crystal with Fibonacci optical superlattices. © 2000 Published by Elsevier Science B.V. All rights reserved.

*PACS:* 42.65.Ky; 42.79.Nv; 42.70.Mp

## 1. Introduction

Efficient third and fourth harmonic generation is usually achieved by using tandem of birefringent phase matched quadratic nonlinear crystal [1,2]. The disadvantage of this method is that only limited number of crystals allow birefringent phase matching. It requires very precise crystal angular or temperature alignment. Special alignment of the polarization planes of the two crystals is necessary for efficient tripling [2]. The efficiency of the process of higher harmonic generation can be greatly increased if instead of consequently situated crystals one can use single nonlinear crystal. The first suggestion about phase-matched third-harmonic generation (THG) in single $\chi^{(2)}$ nonlinear crystal can be found in the book of Akhmanov and Khohlov [3]. Soon it became clear that it is impossible to realize simultaneous birefringent phase matching for two processes except for accidental input wavelengths and non-collinear geometry [4,5]. The last few years the interest towards possibility to generate higher order harmonics in monolithic nonlinear element appeared again. For example, recently a new approach that uses Fibonacci type aperiodic quasi-phase matched (QPM) gratings was successfully applied for achieving simultaneous phase matching for the processes of second harmonic generation and sum frequency mixing and as a result efficient THG in single $LiTaO_3$ crystal [6,7]. An alternative approach for frequency tripling and quadrupling that uses a single crystal

* Corresponding author. E-mail: saltiel@phys.uni-sofia.bg

0030-4018/00/$ - see front matter 
PII: S0030-4018(00)00654-4

QPM gratings was suggested in Ref. [8] and soon realized in GaAs [9]. In the first grating it is generated second harmonic wave, in the second grating is generated third harmonic wave by sum-frequency mixing ($\omega + 2\omega = 3\omega$). In this first not optimized attempt for construction single $\chi^{(2)}$ crystal frequency tripler 0.66% peak power conversion efficiency was achieved. Single periodically poled lithium niobate crystal with two QPM gratings was also employed to realize optical 1-to-3 frequency division [10].

In the last two works it is suggested that the two gratings have to have equal lengths. There is no works considering the optimization of these kind single pass double grating structures. For example it is interesting to define the optimal ratio of the lengths of the two gratings. Such an optimization should lead to increase of the efficiency of these types frequency conversion devices. Additionally there is no work where the two single crystal approaches for THG (Fibonacci grating and double-grating) have been compared.

In this paper we investigate theoretically the process of frequency tripling and quadrupling in double grating QPM structure by using numerical techniques and applying for the first time low depletion approximation [11,12] for description of the cascade second order frequency conversion processes. It is found that the optimal grating length ratio depends on the input intensity and the amount of the effective second order susceptibility in each part of the crystal.

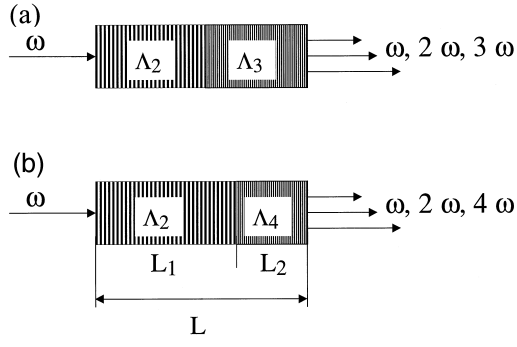


Fig. 1. Schematic of a monolithic double-grating frequency converter for third harmonic (a) and fourth harmonic (b) generation. $\Lambda_2$, $\Lambda_3$ and $\Lambda_4$ are QPM grating periods.

The grating periods and the acceptance (temperature and wavelength) for some nonlinear crystals are also calculated. The comparison of the Fibonacci approach and the double grating approach is presented.

The idea of the double grating frequency tripling and quadrupling is presented in Fig. 1(a) and Fig. 1(b). It is assumed that the QPM grating in the leading part of the crystal is designed to support the process of Type I second harmonic generation (SHG) and the second part of the crystal is patterned for phase matched THG (Fig. 1(a)) by the process of sum frequency mixing $2\omega + \omega = 3\omega$ or forth harmonic generation (Fig. 1(b)) by the process of frequency doubling of the generated in the first part of the crystal second harmonic wave $2\omega + 2\omega = 4\omega$. The second grating can be designed for first or higher-order QPM.

## 2. Plane wave equation systems

Amplitude equations system that describe the process of SHG in the first part of the crystal in suggestion of lossless nonlinear media and plane wave linear polarized input wave has the form

$$\frac{dA_1}{dz} = -i\sigma_1 A_1^* A_2 \exp(-i\Delta k_2 z), \tag{1.1}$$

$$\frac{dA_2}{dz} = -i\sigma_2 A_1^2 \exp(i\Delta k_2 z). \tag{1.2}$$

The process of sum frequency generation $2\omega + \omega = 3\omega$ in the second part of the crystal is described by:

$$\frac{dB_1}{dz} = -i\sigma_3 B_3 B_2^* \exp(-i\Delta k_3 z), \tag{2.1}$$

$$\frac{dB_2}{dz} = -i\sigma_4 B_3 B_1^* \exp(-i\Delta k_3 z), \tag{2.2}$$

$$\frac{dB_3}{dz} = -i\sigma_5 B_1 B_2 \exp(i\Delta k_3 z). \tag{2.3}$$

In the second part of the crystal of the frequency converter shown in Fig. 1(b) is generated fourth harmonic wave. The QPM grating in this part of the

crystal is constructed to phase match only the process $2\omega + 2\omega = 4\omega$. The equation system in this case is

$$\frac{dB_2}{dz} = -i\sigma_6 B_2^* B_4 \exp(-i\Delta k_4 z), \quad (3.1)$$

$$\frac{dB_4}{dz} = -i\sigma_8 B_2^2 \exp(i\Delta k_4 z). \quad (3.2)$$

$A_1$, $B_1$, $A_2$, $B_2$, $B_3$, $B_4$ are the complex amplitudes for the fundamental (subindex 1), second (subindex 2), third (subindex 3), and fourth (subindex 4) harmonic wave respectively They are connected to the real amplitudes and phases by $A_j = a_j \exp(i\varphi_j)$, $j = 1,2$ and $B_j = b_j \exp(i\psi_j)$, $j = 1,2,3,4$. Phase mismatch parameters are as follow: $\Delta k_2 = k_2 - 2k_1 - 2\pi m_1/\Lambda_2$, $\Delta k_3 = k_3 - k_2 - k_1 - 2\pi m_2/\Lambda_3$ and $\Delta k_4 = k_4 - 2k_2 - 2\pi m_2/\Lambda_4$, where $\Lambda_2$ is the QPM grating period of the first part of the crystal $\Lambda_3$ and $\Lambda_4$ are the QPM grating periods for the second part of the crystal for the cases of third and fourth harmonic generation, respectively.

Nonlinear coupling coefficients $\sigma_j$ are proportional to the $d^{(2)}$ value and depend on the order of QPM grating used in any of the part of the crystal:

in the first part of the crystal

$$\sigma_j = \left(\frac{2}{m_1\pi}\right)\frac{2\pi d_{2\omega}^{(2)}}{\lambda_1 n_j}, \quad j = 1,2;$$

in the second part of the crystal

$$\sigma_j = \left(\frac{2}{m_2\pi}\right)\frac{2\pi d_{3\omega}^{(2)}}{\lambda_{j-2} n_{j-2}}, \quad j = 3,4,5$$

and

$$\sigma_j = \left(\frac{2}{m_2\pi}\right)\frac{2\pi d_{4\omega}^{(2)}}{\lambda_2 n_{j-4}}, \quad j = 6,8.$$

The ratios between all $\sigma_j$ depend on dispersion of the nonlinear tensor component $d^{(2)}$ and the dispersion of the index of refraction $n$. The dispersion effect of $d^{(2)}$ is described by the well known Miller rule [13]. As a result we have

$$\sigma_2 = f_2\sigma_1;\ \ \sigma_3 = f_5\sigma_1(m_1/m_2);\ \ \sigma_4 = 2f_2\sigma_3;$$

$$\sigma_5 = 3f_3\sigma_3;\ \ \sigma_6 = 2f_2 f_6\sigma_1(m_1/m_2);$$

$$\sigma_8 = (f_4/f_2)\sigma_6,$$

where

$$f_j = n_1/n_j,\ \ j = 2,3,4;\ \ f_5 = \frac{d_{3\omega}^{(2)}}{d_{2\omega}^{(2)}} = \frac{n_3^2 - 1}{n_1^2 - 1};$$

$$f_6 = \frac{d_{4\omega}^{(2)}}{d_{2\omega}^{(2)}} = \frac{(n_2^2 - 1)(n_4^2 - 1)}{(n_1^2 - 1)^2}.$$

For the cases when the dispersion effects can be neglected all $f_j = 1$.

The terms that are responsible for the other second and third order interactions are omitted. These terms are neglected because they are inefficient due to very high value of the corresponding wave vector mismatches.

There are two possible approaches for exact solution of systems (1)–(3): (i) direct numerical integration; and (ii) analytical formulae expressed in Jacobi elliptic functions and integrals. The use of such kind of analytical formulae is rather difficult since the elliptic sinus and the elliptic integral of the third kind have to be evaluated by complicated numerical calculations. Direct numerical integration is the most popular exact method for investigation of frequency conversion processes. In the same time for preliminary estimation purposes there is a need of approximate analytical formulas that can be used for fast evaluation of the efficiency of the frequency conversion processes. In this paper we apply for the first time approach 'Low depletion approximation' (LDA) for description of the second-order frequency conversion processes. LDA was used for the first time for description of $\chi^{(3)}{:}\chi^{(3)}$ cascade processes in centrosymmetric media [11,12]. LDA has advantages with respect to the known fixed amplitude approximation [14] and fixed intensity approximation (see Ref. [2] and the references therein). LDA is the only approximate method that describes the depletion of

the fundamental waves that is very important when one has to obtain analytical formulas for cascade frequency conversion processes as in our case. Additional argument for using the LDA approach is that it is the only approach that gives correct approximate formulas for the phase shift of the interacting waves.

The details of the derivation of the analytical formulae with LDA are presented in the Appendix.

## 3. Third and fourth harmonic efficiency

Third harmonic efficiency $\eta_{3\omega} = |b_3/a_{10}|^2$ for the device shown in Fig. 1(a) at not very big input intensity, as found with LDA (see the Appendix) is given by the following expression:

$$\eta_{3\omega} = \left(\sigma_5\sigma_2 a_{10}^2 L_2 L_1\right)^2 \left[1 - \left(\sigma_1\sigma_2 a_{10}^2 L_1^2\right) \times \mathrm{sinc}^2(Q_2 L_1)\right] \mathrm{sinc}^2(Q_2 L_1)\,\mathrm{sinc}^2(Q_3 L_2), \tag{4}$$

where

$$Q_2^2 = 2\sigma_1\sigma_2 a_{10}^2 + \Delta k_2^2/4, \tag{5.1}$$

$$Q_3^2 = \sigma_4\sigma_5 a_{10}^2 + \sigma_2\sigma_5(\sigma_3\sigma_2 - \sigma_4\sigma_1) a_{10}^4 L_1^2 \times \mathrm{sinc}^2(Q_2 L_1) + \frac{\Delta k_3^2}{4}. \tag{5.2}$$

Eq. (4) allows to find the efficiency of the THG process and the optimal relative length of the two grating for not so big input intensity that correspond to $\sigma_1 a_{10} L \le 1.2$. As a guide we would like to note that $\sigma_1 a_{10} L = 1.2$ corresponds to input intensities equal to 0.4, 15, 12.7 and 4 MW/cm$^2$ for GaAs, KTP, $LiTaO_3$, $LiNbO_3$, respectively. For higher input intensities the efficiency of THG can be calculated by direct integration of system (1) and (2). For the numerical evaluation with the analytical formulae and the numerical integration of systems (1), (2) and (3) performed in this work we assumed that the ratios between all $\sigma_j$ correspond to an experiment with $\lambda_1 = 1.55$ μm in one of the crystals KTP, $LiNbO_3$ or $LiTaO_3$. The values of $f_j$ used in this work ($f_2$, $f_3$, $f_4$, $f_5$, $f_6$) = (0.98, 0.96, 0.91, 1.12, 1.31) does not deviate from the exact values of $f_j$ for any of the considered crystals with more than 1% (only for $f_6$ the deviation is 3%).

The validity of Eq. (4) is found by direct comparison with the results obtained from exact numerical integration of systems (1) and (2). In Fig. 2(a) is shown the dependence of $\eta_{3\omega}$ as a function of the normalized length of the first grating $L_1/L$ in case of exact phase matching for both interactions. It is seen that LDA can be applied for fundamental input amplitudes up to $\sigma_1 a_{10} L = 1.2$. For these input levels (when $m_1{:}m_2 = 1{:}1$) the conversion into third harmonic is close to 40%, that is bigger than most of the published experimental results.

The dependencies shown in Fig. 2(a) and Fig. 2(b) plotted for exact phase matched conditions show that the optimal relative lengths of the two gratings depend not only on the magnitude of the input fundamental field but also on the order of the QPM gratings. When the two QPM gratings of the frequency tripler are with one and the same order and the normalized input amplitude $\sigma_1 a_{10} L$ is not too high the optimal length of the first grating is $\sim 0.54$ (i.e. the two grating have approximately the same lengths) and remains the same for these magnitudes of the input fundamental field. If, however, the ratio of the orders of the two gratings is $m_1{:}m_2 = 1{:}3$ the optimal length of the gratings strongly depends on the magnitude of the input fundamental field. The higher is the input field the shorter should be the first grating. It is clear that the optimization of the length of the gratings is particularly important when the two QPM gratings are not the same order. In this case the optimization of the length of the gratings can double the conversion efficiency with respect to the case of equal length gratings i.e. the efficiency that corresponds to $L_1/L = 0.5$ (see also Fig. 5).

Fig. 2(c) shows the dependence of third harmonic efficiency at higher values of normalized input amplitude ($\sigma_1 a_{10} L > 1.5$). At this power level the dependence of $\eta_{3\omega}$ on the relative length of the first grating is more complicated and has two maxima. The optimal relative length of the first grating is reducing with the increase of the fundamental field amplitude. This behavior can be explained by noting that the process of THG in the second part of the crystal require optimal ratio for the amplitudes of the fundamental and the second harmonic field. So, at higher values of the input amplitude, the first grating should be shorter in order to prevent strong depleting of the fundamental wave.

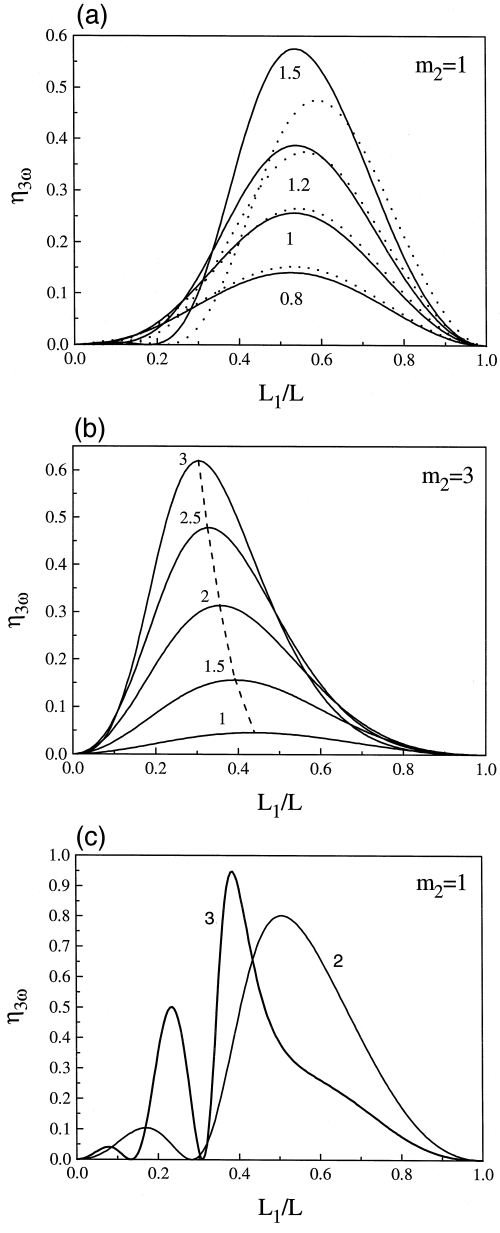


Fig. 2. Third harmonic efficiency against the relative length of the grating for SHG calculated for the case of exact phase matching for both interactions. The parameter is $\sigma_1 a_{10} L$, the normalized input amplitude: (a) both parts of the crystal are patterned with I order QPM gratings. The solid line corresponds to the numerical solution of system (1) and (2); the dotted line represents the approximate solution obtained by LDA approach, Eq. (4); (b) the first parts of the crystal is patterned with I order QPM grating, the second one with III order QPM grating; the dashed line connects the maxima of the curves; and (c) the same as (a), but for $\sigma_1 a_{10} L > 1.5$.

Fourth harmonic efficiency of the converter shown in Fig. 1(b) can be calculated with the use of following approximate analytical formula

$$\eta_{4\omega} = \frac{b_4^2}{a_{10}^2} = \left(\sigma_2^2 \sigma_4 a_{10}^3 L_2 L_1^2\right)^2 \mathrm{sinc}^4(Q_2 L_1)\mathrm{sinc}^2(Q_4 L_2), \quad (6)$$

where

$$Q_4^2 = 2\left(\sigma_2^2 \sigma_4 \sigma_6 a_{10}^4 L_1^2\right)\mathrm{sinc}^2(Q_2 L_1) + \Delta k_4^2/4.$$

The range of the validity of approximation (6) is the same as in the case of THG, $\sigma_1 a_{10} L \le 1.2$. For higher input values we used exact numerical solution of systems (1) and (3). The result of the calculated conversion into fourth harmonic as a function of the relative length of the first grating is shown in Fig. 3(a) and Fig. 3(b). The behavior is the same as for the case of third harmonic generation: constant optimal ratio for the two gratings when $m_1{:}m_2 = 1{:}1$ and reduction of the ratio $L_1/L$ when $m_1{:}m_2 = 1{:}3$. It is important to note that, when the two QPM gratings are the same order, the optimal ratio $L_1/L$ is 0.6 and, as it is seen from Fig. 3(c), remains approximately the same at higher values for the fundamental field. This is in contrast with the behavior of the same dependencies in the case of THG (see Fig. 2(c)).

It is interesting to define if such double-grating converters can be used with tunable lasers, to determine their wavelength and temperature acceptance. For this reason we investigated the conversion efficiency into third harmonic for two converters made from $LiTaO_3$ and $LiNbO_3$ (with parameters given in Table 1) as a function of the input wavelength and the temperature.

Fig. 4 shows the conversion efficiency into third harmonic when the fundamental frequency and the temperature are both deviated from the point of maximum conversion $(\lambda_1, T_0)$. The calculations were made for the fixed normalized input amplitude $\sigma_1 a_{10} L = 1.4$ and the ratio between the length of the two gratings $L_1/L = 1.083$. The wave vector mismatch parameters $\Delta k_2$ and $\Delta k_3$ were calculated with the temperature dependent Selmier equations taken from Ref. [16] for $LiNbO_3$ and from Ref. [15] for $LiTaO_3$.

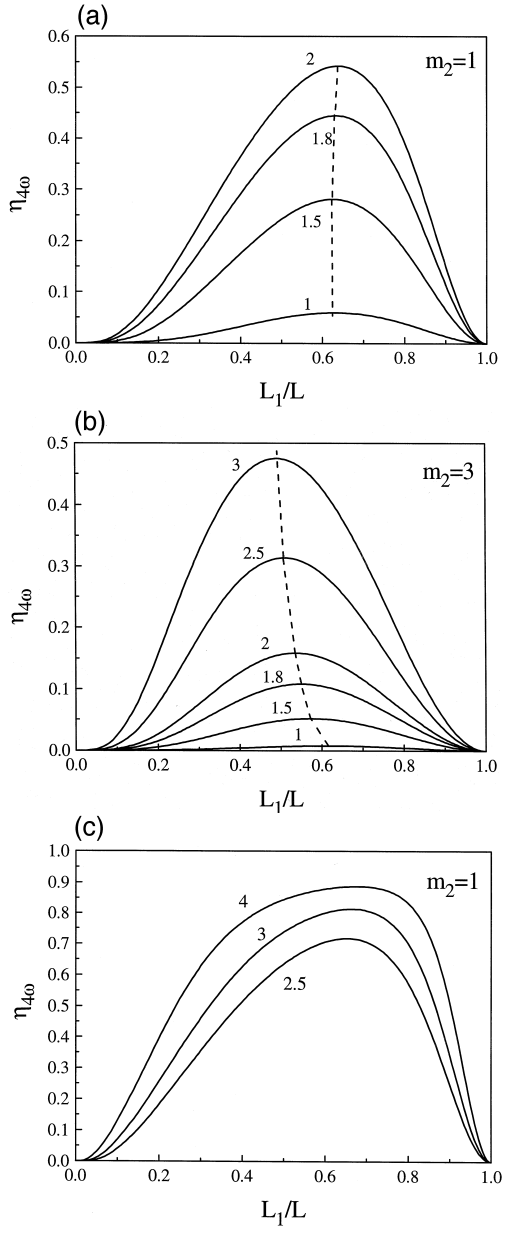


Fig. 3. Fourth harmonic efficiency against the relative length of the grating for SHG as obtained by numerical solution of the systems (1) and (3) in the case of exact phase matching for both interactions. The parameter is $\sigma_1 a_{10} L$, the normalized input fundamental amplitude. The dashed line connects the maxima of the curves: (a) both parts of the crystal are patterned with I order QPM gratings; (b) the first parts of the crystal is patterned with I order QPM grating, the second one with III order QPM grating; and (c) the same as (a), but for $\sigma_1 a_{10} L > 2$.

As can be seen from the figures, $LiTaO_3$ is suitable for tripling the frequency of tunable pumping sources. One double-grating structure with fixed periods in both parts can be used to convert into third harmonic in wavelength region wide as much as 50 nm. In order to keep the phase matching conditions satisfied, the increase of the pumping wavelength require increase of the temperature. Single double-grating structure made on the base of $LiNbO_3$ crystal can be used in wavelength region wide 16 nm, that is three times less than in $LiTaO_3$. The insets in the figures illustrate the magnitude of the temperature and wavelength acceptance of the converters designed with the parameters listed in Table 1. As seen the calculated temperature and wavelength tolerances ($\Delta\lambda = 1.5$ and $\Delta T = 10°$ for $LiTaO_3$ and $\Delta\lambda = 1.1$ nm and $\Delta T = 9°$ for $LiNbO_3$) are easy to satisfy in comparison with the tolerance of the angle phase matched converters.

The dependence of the conversion coefficient $\eta_{3\omega}$ on the input power is shown in Fig. 5. The calculations are done for $LiTaO_3$ as nonlinear media of the double-grating frequency converter. For comparison on the same graph is shown the efficiency when Fibonacci grating is employed. As we discussed in the introduction, nonlinear element with Fibonacci grating is an alternative approach for generation of third or fourth harmonic in single nonlinear crystal [6,7]. Fibonacci QPM grating is constructed from two blocks A and B. Each block consists two layers: the first one has $\chi^{(2)}$ with positive sign and the second one has $\chi^{(2)}$ with negative sign. The consecutive disposition of the blocks follows the rule $S_j = S_{j-1}/S_{j-2}; j \geq 3$, where $S_1 = A$, $S_2 = AB$. The curve shown in Fig. 5 is calculated for the $LiTaO_3$ sample discussed in the publication [6,7] by numerical solution of the equations [3,17]:

$$\frac{dB_1}{dz} = -i\sigma_3 B_3 B_2^* - i\sigma_1 B_2 B_1^*, \tag{7.1}$$

$$\frac{dB_2}{dz} = -i2\sigma_3 B_3 B_1^* - i\sigma_1 B_1^2, \tag{7.2}$$

$$\frac{dB_3}{dz} = -i3\sigma_3 B_1 B_2. \tag{7.3}$$

For the calculation with system (7) following values for the nonlinear coupling coefficients were adopted

Table 1
Parameters for the calculations presented in Fig. 4

| Crystal | $\lambda_1$ (μm) | $T_0$ (°C) | $m_1$:$m_2$ | $\Lambda_2$ (μm) | $\Lambda_3$ (μm) | $d_{33}^{(2)}$ (pm/V) | $P_{in}$ (MW/cm$^2$) |
|---|---|---|---|---|---|---|---|
| LiTaO3 | 1.55 | 150 | 1:1 | 20.238 | 7.636 | 15[a] | 17.3 |
| LiNbO3 | 1.55 | 100 | 1:1 | 18.97 | 6.806 | 27[b] | 5.3 |

[a] Ref. [15].
[b] Ref. [2].

$\sigma_1 = 0.546\sigma_{0,1}$ and $\sigma_3 = \sigma_1/3$ [6,7]. The curves representing three different double-grating structures are calculated by solving systems (1) and (2).

As can be seen from Fig. 5 the optimization of the ratio of the length of the gratings is very important factor for the double-grating elements with different orders QPM in both part of the crystal (compare the dotted and dash–dotted lines that are for ratios $L_1/L = 0.5$ and $L_1/L = 0.3$, respectively. Fig. 5 demonstrates also that the generation of third harmonic in double-grating structures is more efficient than with crystals with Fibonacci gratings. This result does not support the conclusion presented in Ref. [6] that the 'Fibonacci' method for single crystal THG is almost one order of magnitude more efficient than the double grating frequency converter.

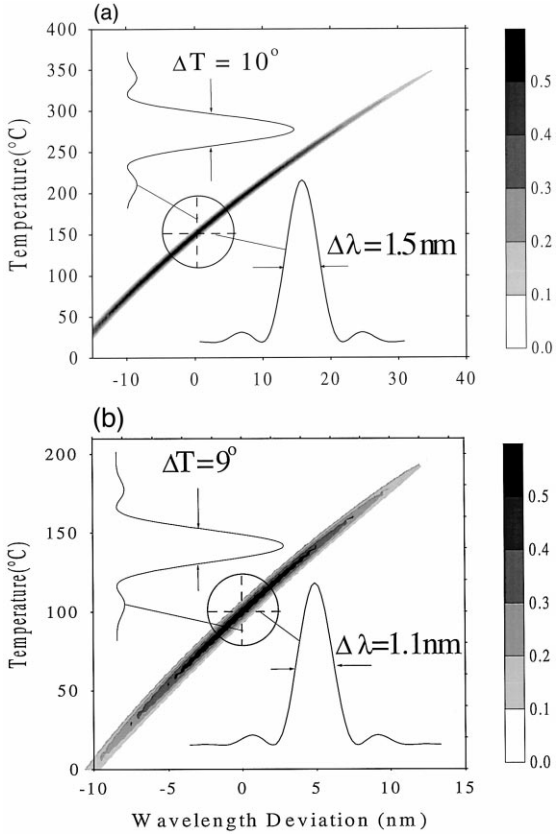


Fig. 4. Third harmonic efficiency of a monolithic double-grating frequency converter made from $LiTaO_3$ crystal (a) and $LiNbO_3$ crystal (b) as a function of the temperature and the deviation $\lambda_1$-$\lambda_{1,0}$ from the central wavelength $\lambda_{1,0} = 1.55$ μm. The normalized input intensity is $\sigma_1 a_{10} L = 1.4$. The length of the crystal $L = 1$ cm. The other parameters are given in Table 1. The insets illustrate the temperature and the wavelength acceptance.

## 4. QPM gratings for $LiNbO_3$, $LiTaO_3$, KTP and GaAs

In this section we present the grating periods for four different crystals. The formula for the dispersion

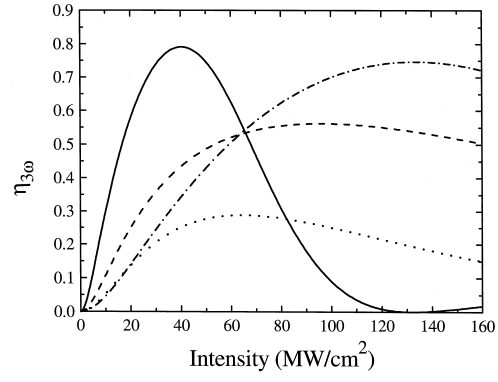


Fig. 5. Comparison of the third harmonic efficiency of three monolithic devices made from $LiTaO_3$ crystal with length $L = 1$ cm for the case of exact phase matching for both interactions. Solid line: double-grating element with $m_1 = 1$, $m_2 = 1$ and $L_1/L = 0.54$. Dotted line: double-grating element with $m_1 = 1$, $m_2 = 3$ and $L_1/L = 0.5$. Dash-dotted line: double-grating element with $m_1 = 1$, $m_2 = 3$ and $L_1/L = 0.3$. Dashed line: nonlinear crystal patterned with Fibonacci optical superlattices [6,7].

of the index of refraction are taken as follow: for $LiNbO_3$ from Ref. [16], for $LiTaO_3$ from Ref. [15], for KTP from Ref. [2], and for GaAs from Ref. [18]. The input polarization is along $z$ axis for all crystals with exception for the GaAs for which the input polarization has [111] direction. Fig. 6(a)–(d) shows the dependence of grating periods $\Lambda_2$, $\Lambda_3$ and $\Lambda_4$, respectively, for second harmonic, third harmonic and fourth harmonic generation, as a function of the input wavelength $\lambda_1$.

With the contemporary level of the technique of production of QPM gratings it is very difficult gratings with periods below 4 μm to be achieved. For the input wavelengths for which the first order QPM grating is below 4 μm, third order QPM grating should be used. However, as it was shown in part III, the use of third order QPM grating in the second part of the crystal will lead to lower conversion into third harmonic for one and the same input power. But by choosing the optimal ratio of the grating lengths the reduction of the conversion efficiency can be partially compensated. The periods of third order of QPM gratings that allow phase matching of the processes $2\omega + \omega = 3\omega$ and $2\omega + 2\omega = 4\omega$ are also shown in Fig. 6(a)–Fig. 6(d).

For certain fundamental wavelengths the two gratings of the devices shown in Fig. 1 have one and the same period (i.e. $\Lambda_2 = \Lambda_3$ or $\Lambda_2 = \Lambda_4$). At these points the two processes are simultaneously phase matched in the whole crystal. Such double-phase matched schemes can be used not only for obtaining efficient third and fourth harmonic generation, but

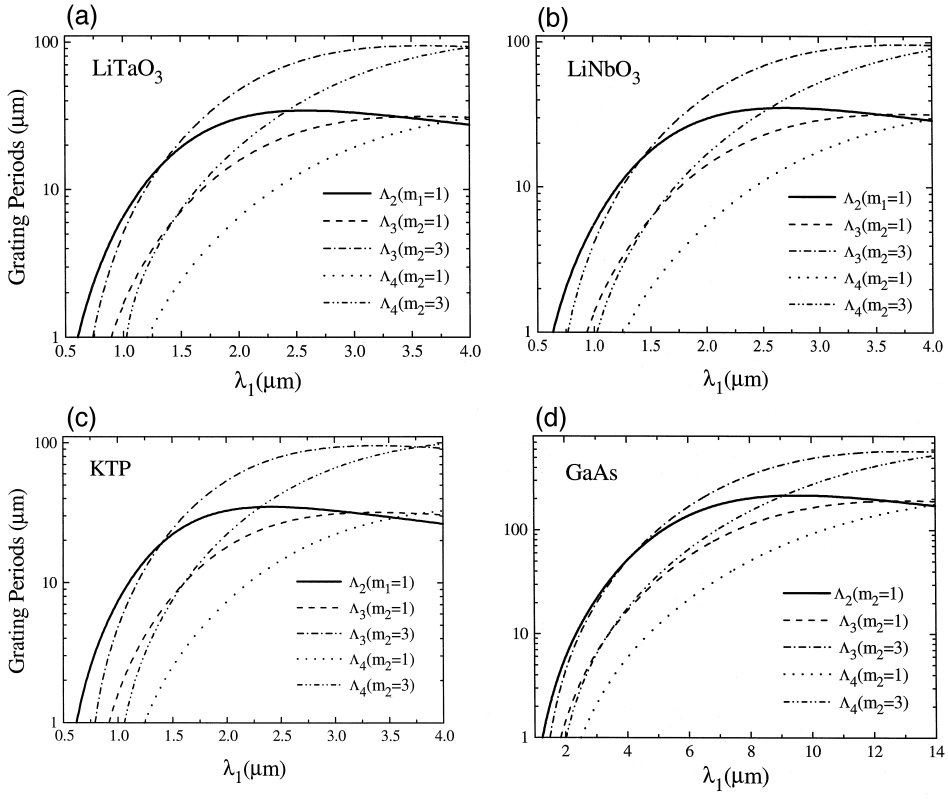


Fig. 6. QPM grating periods $\Lambda_2$, $\Lambda_3$ and $\Lambda_4$ for the processes second harmonic of the fundamental frequency $\omega + \omega = 2\omega$, sum frequency mixing $\omega + 2\omega = 3\omega$, and frequency doubling of the second harmonic radiation $2\omega + 2\omega = 4\omega$ respectively: (a) $LiTaO_3$; (b) $LiNbO_3$; (c) KTP; and (d) GaAs.

also for obtaining large nonlinear phase shift [17,19], polarization switching [20] and multidimensional solitary waves [21,22].

## 5. Conclusion

The optimal conditions for third and fourth harmonic generation in nonlinear crystals with double-grating QPM patterns was investigated theoretically. It is found the optimal length of the two gratings. At relatively low input power the output parameters of this types of the frequency converters can be correctly described by the analytical formula obtained in the frame of the low depletion approximation. It is shown that this double grating frequency tripler is more efficient than the method of frequency tripling in crystals with Fibonacci gratings. We believe that the results obtained in this work will allow to construct compact diode pumped frequency converters.

## Acknowledgements

S.S. thanks M. Fejer, G. Imeshev and I. Lambrev for the very useful discussions. The support of Bulgarian Science Foundation with grant F-803 is acknowledged.

## Appendix A

The aim of this Appendix is to outline the derivation of the analytical formula for description of the double-grating frequency converters. For this purpose we extend recently introduced in Refs. [11,12] low depletion approximation (LDA) by applying this approach for description of such second-order processes as second harmonic generation and sum frequency mixing.

### *A.1. SHG in the first part of the crystal*

First of all let us apply the LDA to the case of second harmonic generation. System (1) can be rewritten for the real amplitudes and phases of the interacting waves:

$$\frac{\mathrm{d}a_1}{\mathrm{d}z} = \sigma_1 a_2 a_1 \sin\Phi_1, \tag{A1.1}$$

$$\frac{\mathrm{d}a_2}{\mathrm{d}z} = -\sigma_2 a_1^2 \sin\Phi_1, \tag{A1.2}$$

$$\frac{\mathrm{d}\varphi_1}{\mathrm{d}z} = -\sigma_1 a_2 \cos\Phi_1, \tag{A1.3}$$

$$\frac{\mathrm{d}\varphi_2}{\mathrm{d}z} = -\sigma_2 \frac{a_1^2}{a_2} \cos\Phi_1, \tag{A1.4}$$

where

$$\Phi_1 = \varphi_2 - 2\varphi_1 - \Delta k_2 z.$$

The two invariants of system (4) are:

$$a_1^2 + \frac{\sigma_1}{\sigma_2} a_2^2 = a_{10}^2 + \frac{\sigma_1}{\sigma_2} a_{20}^2 = u^2, \tag{A2}$$

$$\sqrt{\sigma_1}\, a_1^2 a_2 \cos\Phi_1 + \Delta k_2 \sigma_1 a_2^2 / 2\sqrt{\sigma_1}\, \sigma_2 = \Gamma, \tag{A3}$$

where $a_{j0}$ are the input amplitude for the interacting wave. In case of no second harmonic seeding $\Gamma = 0$ and $u^2 = a_{10}^2$.

Expressing $\sin\Phi$ from (A3) and substituting in (A1.2) we obtain

$$\frac{\mathrm{d}a_2^2}{\mathrm{d}z} = -2a_{10}^3 \sqrt{\sigma_2^2 \left(\frac{a_2}{a_{10}}\right)^2 - \frac{Q_2^2}{a_{10}^2}\left(\frac{a_2}{a_{10}}\right)^4 + \sigma_1^2 \left(\frac{a_2}{a_{10}}\right)^6}, \tag{A4}$$

where

$$Q_2^2 = 2\sigma_1 \sigma_2 a_{10}^2 + \frac{\Delta k_2^2}{4}.$$

For relatively low conversion the term $(a_2/a_{10})^6$ can be neglected and integration of (A4) leads to:

$$a_2 = \left(\sigma_2 a_{10}^2 L_1\right) \mathrm{sinc}\left(Q_2 L_1\right), \tag{A5.1}$$

$$a_1 = a_{10} \sqrt{1 - \left(\sigma_1 \sigma_2 a_{10}^2 L_1^2\right) \mathrm{sinc}^2\left(Q_2 L_1\right)}. \tag{A5.2}$$

The output phases $\varphi_1$ and $\varphi_2$ for the fundamental and second harmonic wave at the interface between the two gratings are obtained by integration of (A1.3)

and (A1.4)

$$\varphi_1(L_1) = \varphi_{10} - \frac{\Delta k_2 L_1}{2}\frac{\sigma_1}{\sigma_2} + \frac{\Delta k_2}{2}\frac{\sigma_1}{\sigma_2}\frac{\operatorname{atan}\left[\sqrt{1-2M_2}\tan(Q_2 L_1)\right]}{Q_2\sqrt{1-2M_2}}. \quad \text{(A6.1)}$$

$$\varphi_2(L_1) = \frac{\Delta k_2 L_1}{2}, \quad \text{(A6.2)}$$

where

$$M_2 = \frac{1}{2}\frac{\sigma_2^2 a_{10}^2}{Q_2^2}.$$

The expressions (A5.1) and (A5.2) describe second harmonic amplitude and the fundamental wave amplitude as a function of the input field, length of the grating and the wave vector mismatch. It is interesting to note that Eq. (A6.1) describes the stepwise behaviour of the fundamental wave nonlinear phase shift as a function of the input field and the length of the media.

The amplitudes and phases $a_j(L_1)$, $\varphi_j(L_1)$, ($j = 1,2$) will be used as input waves for the calculation third (fourth) harmonic efficiency in the second part of the crystal.

*A.2. Sum frequency generation in the second part of the crystal*

System (2) when written separately for the amplitudes and the phases of the interacting waves has the form:

$$\frac{db_1}{dz} = \sigma_3 b_3 b_2 \sin\psi, \quad \text{(A7.1)}$$

$$\frac{db_2}{dz} = \sigma_4 b_3 b_1 \sin\psi, \quad \text{(A7.2)}$$

$$\frac{db_3}{dz} = -\sigma_5 b_1 b_2 \sin\psi, \quad \text{(A7.3)}$$

$$\frac{d\psi_1}{dz} = -\sigma_3\frac{b_3 b_2}{b_1}\cos\psi, \quad \text{(A7.4)}$$

$$\frac{d\psi_2}{dz} = -\sigma_4\frac{b_3 b_1}{b_2}\cos\psi, \quad \text{(A7.5)}$$

$$\frac{d\psi_3}{dz} = -\sigma_5\frac{b_1 b_2}{b_3}\cos\psi, \quad \text{(A7.6)}$$

where $\psi = \psi_3 - \psi_2 - \psi_1 - \Delta k_3 z$. The invariants of system (7) in the case of no third harmonic wave at the entrance of the second part of the crystal are:

$$\sigma_5 b_1^2 + \sigma_3 b_3^2 = \sigma_5 a_1^2,$$

$$\sigma_5 b_2^2 + \sigma_4 b_3^2 = \sigma_5 a_2^2, \quad \text{(A8.1)}$$

$$b_1 b_2 b_3 \cos\psi + \frac{\Delta k_3}{2\sigma_b} b_3^2 = 0, \quad \text{(A8.2)}$$

where $a_1$ and $a_2$ are output amplitudes for the fundamental and second harmonic wave at the end of the first part of the crystal.

After integration of (A7.1)–(A7.3) we obtain for the amplitude of the fundamental, second and third harmonic wave at the output of the crystal

$$b_3(L_2) = \frac{\sigma_5}{Q_3} a_1 a_2 \sin(Q_3 L_2), \quad \text{(A9.1)}$$

$$b_1^2(L_2) = a_1^2\left(1 - \sigma_3\sigma_5 a_2^2 L_2^2 \operatorname{sinc}^2(Q_3 L_2)\right), \quad \text{(A9.2)}$$

$$b_2^2(L_2) = a_2^2\left(1 - \sigma_4\sigma_5 a_1^2 L_2^2 \operatorname{sinc}^2(Q_3 L_2)\right), \quad \text{(A9.3)}$$

where

$$Q_3^2 = a_1^2\sigma_4\sigma_5 + a_2^2\sigma_3\sigma_5 + \frac{\Delta k_3^2}{4}.$$

Combining ((A9.1)–(A9.3)) and (A5.1), (A5.2) is obtained the Eq. (4) for the efficiency of the THG process.

*A.3. Fourth harmonic generation in the second part of the crystal*

Performing the same transformations as in part A.1 we obtain for the amplitudes of the second and fourth harmonic wave at the output of the second part of the crystal:

$$b_2(L_2) = a_2\sqrt{1 - \sigma_6\sigma_4 a_2^2 L_2^2 \operatorname{sinc}^2(Q_4 L_2)} \quad \text{(A10.1)}$$

$$b_4(L_2) = \sigma_6 a_2^2 L_2 \operatorname{sinc}(Q_4 L_2), \quad \text{(A10.2)}$$

where

$$Q_4^2 = 2\sigma_4\sigma_6 a_2^2 + \frac{\Delta k_4^2}{4}.$$

Eq. (6) is obtained by combining expressions (A10.1)–(A10.2) and (A5.1).

## References


[1] W. Koechner, Solid-state Laser Engineering, 3rd ed., Springer Series in Optical Sciiences, vol. 1, Springer, Berlin, 1992.
[2] V.G. Dmitriev, G. Gurzadyan, D.N. Nikogosyan, Handbook of Nonlinear Optical Crystals, 2nd ed., Springer Ser. Opt. Sci. vol. 64, Springer, Berlin, 1997.
[3] S.A. Akhmanov, R.V. Khokhlov, Problems in Nonlinear Optics, Akad. Nauk USSR, Moscow, 1964, English Edition 1973, Gordon and Breach, New York, 1973.
[4] A.P. Sukhorukov, I.V. Tomov, Izv. Vyssh. Uchebn. Zaved. Radiofiz. 13 (1970) 267.
[5] R.U. Orlov, A.P. Sukhorukov, I.V. Tomov, Annu. Sofia Univ. Phys. 65 (1972) 283.
[6] S. Zhu, Y. Zhu, N. Ming, Science 278 (1997) 843.
[7] Y. Qin, Y. Zhu, S. Zhu, N. Ming, J. Appl. Phys. 84 (1998) 6911.
[8] D. Taverner, P. Britton, P.G.R. Smith, D.J. Richardson, G.W. Ross, D.C. Hanna, Opt. Lett. 23 (1998) 162.
[9] L. Becouarn, E. Lallie, M. Brevignon, J. Lehoux, Opt. Lett. 23 (1998) 1508.
[10] P.T. Nee, N.C. Wong, Opt. Lett. 23 (1998) 46.
[11] S. Saltiel, K. Koynov, P. Tzankov, A. Boardman, S. Tanev, Phys. Rev. A 57 (1998) 3028.
[12] S. Saltiel, K. Koynov, K. Kirov, K. Petrova, J. Opt. Soc. Am. B 16 (1999) 262.
[13] R.C. Miller, Appl. Phys. Lett. 5 (1964) 17.
[14] J.A. Amstrong, N. Blombergen, J. Ducuing, P.S. Pershan, Phys. Rev. 127 (1962) 1918.
[15] J.P. Meyen, M.M. Fejer, Opt. Lett. 22 (1997) 214.
[16] D.H. Jundt, Opt. Lett. 22 (1997) 1553.
[17] K. Koynov, S. Saltiel, Opt. Commun. 152 (1998) 96.
[18] C.M. Bass (Ed.), Handbook of Optics, vol. II, Devices, Measurements and Properties, McGraw-Hill, New York.
[19] S. Saltiel, K. Koynov, Y. Deyanova, Yu.S. Kivshar, J. Opt. Soc. Am. B (2000), in press.
[20] S. Saltiel, Y. Deyanova, Opt. Lett. 24 (1999) 1296.
[21] Yu.S. Kivshar, T.J. Alexander, S. Saltiel, Opt. Lett. 24 (1999) 759.
[22] Yu.S. Kivshar, A.A. Sukhorukov, S.M. Saltiel, Phys. Rev. E 60 (1999) 5056.